



HAL
open science

Bias controlled electrostrictive longitudinal resonance in X-cut lithium niobate thin films resonator

M. Pijolat, C. Deguet, C. Billard, D. Mercier, A. Reinhardt, M. Aïd, S. Ballandras, E. Defaÿ

► **To cite this version:**

M. Pijolat, C. Deguet, C. Billard, D. Mercier, A. Reinhardt, et al.. Bias controlled electrostrictive longitudinal resonance in X-cut lithium niobate thin films resonator. *Applied Physics Letters*, 2011, 98 (23), pp.232902. 10.1063/1.3598410 . hal-00611487

HAL Id: hal-00611487

<https://hal.science/hal-00611487>

Submitted on 4 May 2021

HAL is a multi-disciplinary open access archive for the deposit and dissemination of scientific research documents, whether they are published or not. The documents may come from teaching and research institutions in France or abroad, or from public or private research centers.

L'archive ouverte pluridisciplinaire **HAL**, est destinée au dépôt et à la diffusion de documents scientifiques de niveau recherche, publiés ou non, émanant des établissements d'enseignement et de recherche français ou étrangers, des laboratoires publics ou privés.



Distributed under a Creative Commons Attribution 4.0 International License

Bias controlled electrostrictive longitudinal resonance in X-cut lithium niobate thin films resonator

M. Pijolat,¹ C. Deguet,¹ C. Billard,¹ D. Mercier,¹ A. Reinhardt,¹ M. Aïd,¹ S. Ballandras,² and E. Defay^{1,a)}

¹CEA-LETI, Minatec Campus, 38054 Grenoble, France

²FEMTO-ST, UMR 6174, CNRS-UFC-ENSMM-UTBM, 25044 Besançon, France

In this letter, we show that a longitudinal acoustic wave can be generated in X-cut LiNbO₃ (LNO) thin films when a voltage bias is superimposed to the radio frequency signal. Although there is normally no coupling of this wave in X-cut LNO, its electrostrictive behavior combined with bias reaching 3.9 MV/cm induces an electromechanical coupling around 11%. This experiment was performed without acoustic isolation with the LNO substrate (high overtone bulk acoustic resonator configuration).

Acoustic resonators based on piezoelectric substrates and thin films are nowadays extensively utilized for radio frequency (RF) filters. As an example, each mobile phone contains several RF filters that are in turn constituted by approximately ten acoustic resonators each. Two different technologies are developed for such resonators namely surface acoustic wave (SAW) resonators needing piezoelectric substrates and bulk acoustic wave (BAW) resonators based on piezoelectric thin films. The main advantages of SAWs are a rather simple technology with only one lithography level (without considering packaging) and a versatile range of applications thanks to the choice of substrate cuts. Indeed, the piezoelectric materials used for SAW are single crystals of Lithium Niobate (LNO) and Lithium Tantalate (LTO). They both belong to the $3m$ point group below their Curie temperature (T_C). Thus, this induces an intrinsic anisotropy of their macroscopic properties. This behavior gives the opportunity to change the characteristic of the generated surface waves. This is obtained by using different cuts of the single crystal ingots. On the other hand, BAWs can be developed on standard silicon substrates, giving the opportunity to be part of the main stream microelectronic technology. Moreover, since they are based on bulk waves, the thickness of the piezoelectric film is the main parameter to adjust the resonance frequency. This can play a key role for devices requiring frequencies higher than 5 GHz, hardly achievable with SAWs. Aluminum Nitride (AlN) is the foremost piezoelectric material used for this purpose. Indeed, it exhibits a large enough electromechanical coupling, namely 7% together with very low acoustic and dielectric losses to compete with its SAWs counterparts. However, though AlN belongs to the $6mm$ point group, one cannot take advantage of different orientations to adjust its properties as AlN thin films only grow with its c -axis perpendicular to the substrate so far. Few letters are dedicated to inclined growth of AlN, and there are no practical solutions to do so in a large scale.¹ Moreover, AlN for BAWs exhibits a polycrystalline structure, whereas single crystals are highly desired to improve the material quality (no grain boundaries, no misorientation). Therefore, it could be interesting to combine advantages from SAW and BAW approaches. An interesting approach

toward this target is transferring single crystals thin films on a host substrate as already proposed with LNO on LNO (Ref. 2) and LNO on Si.³ LNO is particularly interesting as large single crystal wafers are available (150 mm) with plenty of different crystalline orientations. Moreover, in its ferroelectric state it exhibits only one possibility for the polarization direction, avoiding non-180° domains and consequently energy dissipation due to domain wall motion compared to the closely related perovskite materials as Pb(Zr,Ti)O₃.⁴ Finally, electromechanical coupling coefficients of its bulk waves are high and can even reach 45%.⁵

In this context, we are interested in single crystals X-cut LNO thin films transferred on another LNO substrate. In this letter, we discovered that despite having a null piezoelectric coefficient in the longitudinal direction, a longitudinal thickness mode is excited in the LNO X-cut thanks to the electrostrictive (E) effect that takes place when a dc bias is applied across the LNO thin film. It is worth noting that the coupling coefficient reaches 11% as exposed later on.

Single crystals thin films can be obtained by using a transfer process based on ion implantation/molecular bonding on host substrate/blistering by heating. This technique, called Smart Cut™ has been recently adapted from silicon on insulator (SOI) purposes to LNO thin films onto LNO carrier substrate in collaboration with SOITEC.² Another specificity of this study is that the carrier substrate remains during all experiments as no acoustic isolation is provided. Therefore, in the following, we will be focused on the dc-controlled high overtone bulk acoustic resonator (so-called HBAR) behavior of LNO single crystals thin films transferred on LNO substrate. The technology used to perform the sample is described elsewhere.² Thin film and substrate are both X-Cut LNO and are sketched in inset of Fig. 1. The transferred film is 450 nm thick. Handle and donor wafers are both full 3 inch LNO wafers. The bottom electrode (Mo 150 nm) was sputtered on the handle wafer. Bonding was achieved between two SiO₂ layers deposited, respectively, on the metallic layer and the handle wafer. The sputtered top electrode is made of Al (500 nm thick). The device under test corresponds to a metal insulator metal configuration. RF characterization is performed by using a vector network analyzer. dc field is superimposed to the RF signal.

^{a)}Electronic mail: edefay@cea.fr.

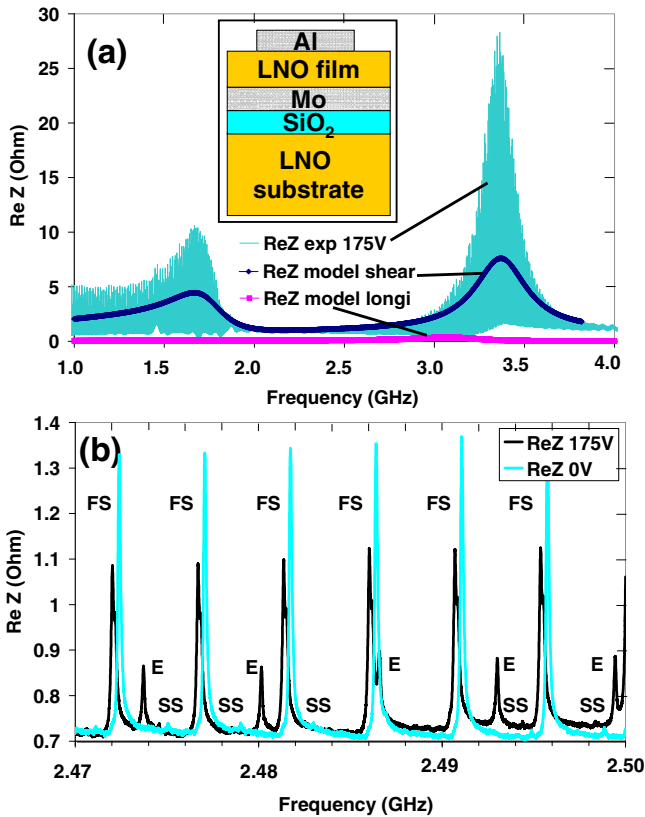


FIG. 1. (Color online) (a) Experimental and models of the real part of the impedance of the HBAR device with 175 V bias superimposed to the RF signal presented in a large frequency range. “Model shear” and “model longi” take into account, respectively, the piezoelectric fast shear (FS) wave alone and the electrostrictive (E) longitudinal wave alone. For sake of clarity, model only fits the average of the curve and not all HBAR peaks. Inset: schematic of the cross section of the HBAR resonator. (b) Experimental of the real part of the impedance of the resonator vs frequency at 0 and 175 V bias presented in a narrow frequency range between 2.47 and 2.50 GHz (FS, SS, and E wave).

Figure 1(a) shows the experimental and modeled real part of impedance (ReZ) of the resonator on a large frequency range, between 1 and 4 GHz biased at 175 V. A lot of sharp peaks are individually hardly ever visible here. Each of them is antiresonance (ReZ considered here) from harmonics of substrate bulk wave modes. All these peaks draw another much broader antiresonance due to the LNO thin film alone. This is typical for HBAR devices.³ As described by Lakin, HBAR electrical behavior can be modeled analytically by considering basic piezoelectric equations and acoustic propagation.⁶ It is worth noting that this model considers one unique mode at a time, as one has to specify the acoustic velocity of the traveling wave. In Fig. 1(a), the model first takes into account the fast shear (FS) wave of X-cut LNO, labeled “ReZ model shear.” As detailed later on, its velocity (4670 m/s) is actually extracted from successive HBAR harmonics obtained through narrow frequency range measurements, as depicted in Fig. 1(b) and labeled FS. For sake of figure clarity, model only fits the average of the experimental curve in Fig. 1(a) and not all HBAR sharp peaks. It is worth noting that on this scale there is no obvious difference between this curve and the one performed without bias (not represented here). Therefore, on this large scale, the FS wave is the only visible as its coupling (estimated higher than 35% here) is much larger than any other wave. To strengthen this statement, we represented the modeled electrostrictive E lon-

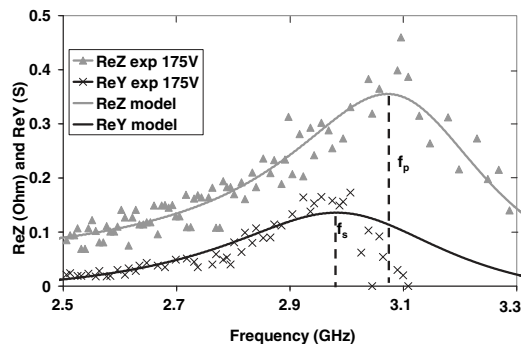


FIG. 2. Amplitude of the real parts of impedance (ReZ) and admittance (ReY) of the E longitudinal wave generated in LNO HBAR by 175 V bias. Each point represents the difference between one E-HBAR peak and the floor value. The Mason model used is fitted by adjusting only the electro-mechanical coupling.

gitudinal mode in Fig. 1(a) (so-called “ReZ model longi”) as obtained from our final analysis (cf. Fig. 2). One can instantaneously observe that this dc-enhanced longitudinal mode is small compared to the piezoelectric FS one. However, the narrow band characterization exhibits evidence of other waves’ presence when bias is on as shown in Fig. 1(b). Three different waves are evidenced: FS, slow shear (SS), and more interestingly E. This last is evidenced only when bias is on [see Fig. 1(b)].

Although the nature of FS and SS peaks is well identified, E type is not common. The frequency distance between two substrate peaks (Δf) is linked to the sound velocity v and the substrate thickness t_s by $v = 2t_s \Delta f$. Therefore, if one assumes the wave propagation and the resonance frequencies are mainly influenced by the substrate, v_E extracted from E type gives $v_E = 6550 \text{ m s}^{-1}$. As $v = \sqrt{c^D / \rho}$ (with c^D the stiffness coefficient and ρ the density [4630 kg/m³ for LNO]), one deduces $c^D = 1.99 \cdot 10^{11} \text{ N/m}^2$. This value corresponds to X-cut c_{33}^D . Therefore, this sound velocity proves dc voltage in LNO induces a longitudinal acoustic wave which is not coupled in X-cut while its corresponding piezoelectric constant is zero. The longitudinal coupling is possible here as dc voltage is combined to the second order electromechanical coupling so-called electrostriction. One can observe in Fig. 1(b) that the FS peak height decreases and experiences a tiny shift toward lower frequency (typical 1.9 MHz) when bias is on. Q factors of such a stack can reach 45 000 for this FS wave.³ It is worth noting that this large Q factor is mainly due to the substrate acoustic quality and not to the active LNO thin film. For E HBAR waves [cf Fig. 1(b)], one can extract roughly $Q = 9000$ if one gets rid of the plateau value of ReZ. However, as we will see later on, the frequency considered here does not correspond to the maximum of the E coupling where the Q value is supposed to be the highest. Besides, one should consider the accuracy a of the applied dc voltage which is typically 0.02% as given by the supplier. If one considers that the corresponding quality factor Q_S of this voltage supply is roughly $1/a$, than $Q_S = 5000$. The height drop of FS is likely to be due to this dc supply effect as well.

As observed in Fig. 1(b), E peaks are clearly visible. Therefore, it should be possible to extract the height of each E peak for ReY and ReZ and to report them on a graph to try to extract the coupling factor of this E wave. This is what is shown in Fig. 2, together with the fitted Mason HBAR model.⁶ Indeed, even if the accuracy of this technique is not

optimal, this procedure leads to a rather acceptable diagram proving the separation of resonance and antiresonance peaks. As suggested by Fig. 1(a), extraction becomes more complicated when one reaches 3 GHz as this corresponds to the highly coupled frequency range of the FS wave. By fitting the Mason model to this experiment, the extracted E electro-mechanical coupling factor k^2 of the LNO film alone reaches 11% with 175 V bias, corresponding to 3.9 MV/cm. The accuracy of this estimation lies around 20%. This coupling can be considered as rather large as it reaches quite half the maximum coupling that the longitudinal wave can experience in LNO for the most appropriated cut [k^2 longitudinal max $\sim 25\%$ (Ref. 5)]. Besides, it is not possible to extract a meaningful Q factor of LNO thin film alone in this HBAR configuration. The next step to reach this goal is to release the LNO thin film from its substrate, which is in itself a serious technological challenge. This E coupling coefficient is larger than the one exhibited by standard E thin films belonging to the perovskite family in the paraelectric phase, namely (Ba,Sr)TiO₃ (6%) (Ref. 7) or SrTiO₃ (3%).⁸ A clear statement on this should be affordable by releasing the LNO thin film.

In this letter, we showed that a longitudinal acoustic wave can be generated in X-cut LNO thin films by applying a bias voltage whereas only shear waves are normally coupled in X-cut LNO. By selecting all the E peaks, we

extracted the coupling coefficient of this bias-controlled wave reaching 11%. This property can be of great interest for switchable RF resonators or filters, if one is able to favor this E resonance far from the piezoelectric resonance. Other LNO orientations could be of interest for this purpose. The next technological step is to release the LNO thin film from the substrate in order to provide a more in-depth assessment on this idea.

¹F. Martin, M. E. Jan, S. Rey-Mermet, D. Su, P. Muralt, and M. Cantoni, Proc.-IEEE Ultrason. Symp. **1-4**, 333 (2005).

²J. S. Moulet, M. Pijolat, J. Dechamp, F. Mazen, A. Tauzin, F. Rieutord, A. Reinhardt, E. Defay, C. Deguet, B. Ghyselen, L. Clavelier, M. Aid, S. Ballandras, and C. Mazuré, *Proceedings of the International Electron Devices Meeting* (IEEE, New York, 2008), p. 679.

³M. Pijolat, S. Loubriat, S. Queste, D. Mercier, A. Reinhardt, E. Defay, C. Deguet, L. Clavelier, H. Moriceau, M. Aid, and S. Ballandras, Appl. Phys. Lett. **95**, 182106 (2009).

⁴J. Conde and P. Muralt, IEEE Trans. Ultrason. Ferroelectr. Freq. Control **55**, 1373 (2008).

⁵G. Kovacs, M. Anhom, H. E. Engan, G. Visintini, and C. C. W. Ruppel, Proc.-IEEE Ultrason. Symp. **1990**, 435.

⁶K. M. Lakin, G. R. Kline, and K. T. Mc Carron, IEEE Trans. Microwave Theory Tech. **41**, 2139 (1993).

⁷A. Noeth, T. Yamada, V. O. Sherman, P. Muralt, A. K. Tagantsev, and N. Setter, J. Appl. Phys. **102**, 114110 (2007).

⁸A. Volatier, E. Defay, M. Aid, A. Nhari, P. Ancey, and B. Dubus, Appl. Phys. Lett. **92**, 032906 (2008).